

Numerical simulation of three-stage water-based CPC operation

Assumption

1. Water vapor through a cylindrical growth tube is described by the energy equation of a Newtonian fluid under steady laminar flow conditions.
2. The particle flow is assumed to be an incompressible Newtonian fluid with a fully developed parabolic flow profile: $v_z(r) = v_0 \left(1 - \frac{r^2}{R^2}\right) = v_0(1 - x^2)$, where v_0 , r , and R represent initial velocity (m/s), radial position (mm), and growth tube radius, respectively, and x is the dimensionless length.
3. Axial thermal diffusion and other second-order effects such as Stefan flow are ignored.

Simplified 1-D heat and mass transfer

The 1-D heat transfer: a partial differential equation of steady laminar flow:

$$v_0 \left(1 - \frac{r^2}{R^2}\right) \frac{\partial T}{\partial z} = D_{th} \left[\frac{1}{r} \frac{\partial}{\partial r} \left(r \frac{\partial T}{\partial r} \right) + \frac{\partial^2 T}{\partial z^2} \right] \quad (1)$$

D_{th} is the thermal diffusivity of the air, 0.215 cm²/sec at STP. At the other operation condition

The 1-D mass transfer: a partial differential equation for partial vapor pressure:

$$v_0 \left(1 - \frac{r^2}{R^2}\right) \frac{\partial P_{va}}{\partial z} = D_{va} \left[\frac{1}{r} \frac{\partial}{\partial r} \left(r \frac{\partial P_{va}}{\partial r} \right) + \frac{\partial^2 P_{va}}{\partial z^2} \right] \quad (2)$$

D_{va} is the mass diffusivity of the water vapor, 0.251 cm²/sec (0.21 by Steve) at STP. At the other operation condition, $D_{va,P} = D_{va}/(P/1(atm)) * \left(\frac{T}{273}\right)^{1.94}$.

The relative humidity or saturation ratio is defined as the ratio of the partial pressure of water vapor (P_{va}) to the equilibrium saturated vapor pressure of water ($P_{sat,T}$) at a given temperature:

$$S = RH = \frac{P_{va}}{P_{sat,T}} \quad (3)$$

The saturated water vapor pressure can be calculated using Antoine equation: $P_{sat,T} = 10^{(A-B/(T+C))}$

$A = 10.1962$, $B = 1730.63$, $C = -39.724$, and T is the temperature in K, and P is the pressure in Pa.

Thus, the above equation can be converted to:

$$v_0 \left(1 - \frac{r^2}{R^2}\right) \frac{\partial S}{\partial z} = D_{va} \left[\frac{1}{r} \frac{\partial}{\partial r} \left(r \frac{\partial S}{\partial r} \right) + \frac{\partial^2 S}{\partial z^2} \right] \quad (4)$$

Simulation condition

1. The growth tube diameter is 6.3 mm ($R=3.15$ mm);
2. The conditioner, initiator and moderator tubing lengths are 73 mm, 30 mm, and 73 mm;
3. Inlet conditions: T_0 , P_0 is the partial water vapor pressure at T_0 .
4. Wall conditions: T_{w1} , T_{w2} , and T_{w3} , and corresponding P_{w1} , P_{w2} , and P_{w3} .

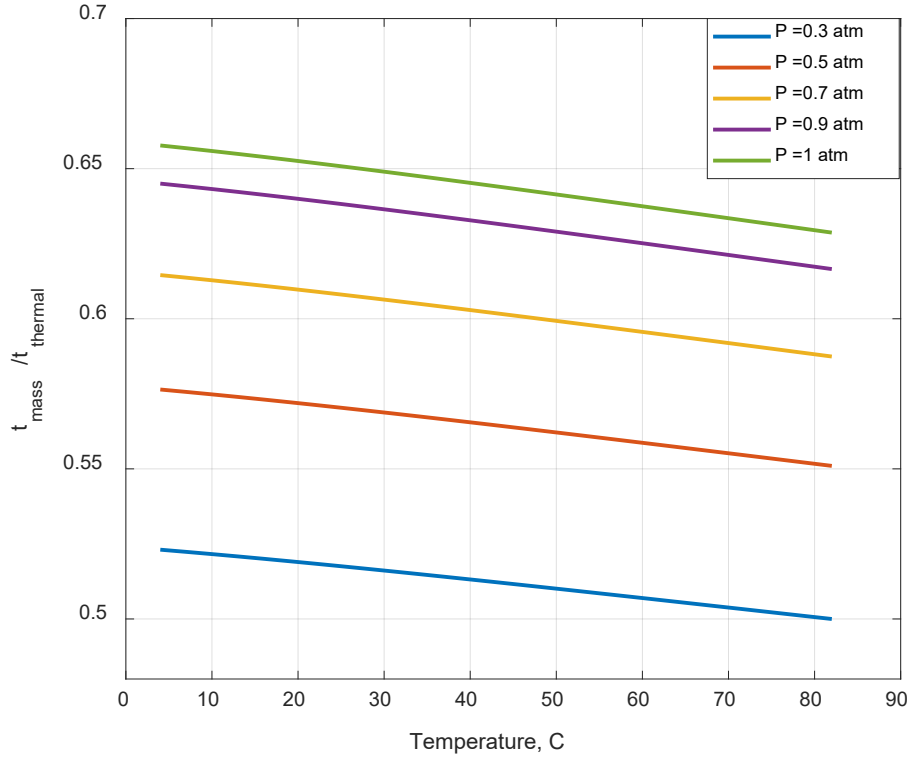


Figure S1. Lewis number as a function of temperature under different operating pressure

Although the configuration of CPC 3789 is different from the previous studies, two fundamental characteristic times can describe how fast the thermal diffusion and the mass diffusion processes will proceed.

$$\tau_{thermal} = \frac{r^2}{D_{th}} = \frac{r^2}{k_a / \rho_a c_p} \quad (1)$$

$$\tau_{mass} = \frac{r^2}{D_{va}} \quad (2)$$

The ratio of those two characteristic times can be designated as the ratio of the thermal diffusivity to the molecular diffusivity of mass, which is also called the Lewis number.

$$Le = \tau_{mass} / \tau_{thermal} = \frac{D_{th}}{D_{va}} = \frac{k_a}{D_{va} \times \rho_a \times c_p} \quad (3)$$

Where r is the radius of the growth tubing, D_{th} is the thermal diffusivity of the air and mainly a function of temperature. D_{va} is the mass diffusivity of the water vapor, which depends on the pressure and temperature, as detailed in the supplement. (Seinfeld and Pandis, 2016)

Based on the dimensionless analysis in Fig. S1, with the decrease of the operation pressure, the Lewis number decreases, which means that the difference between the mass transfer rate and the thermal transfer rate increased with the decrease of the operating pressure. Because the current numerical model and theoretical analysis do not predict this observation, if we assume the water depletion and condensational heat release are negligible, two factors most likely contribute to the counting efficiency

decreases under the low-pressure condition: the significant loss inside the growth tube (wall effect or through the focusing nozzle) and the insufficient droplet growth inside the three-stage tube.

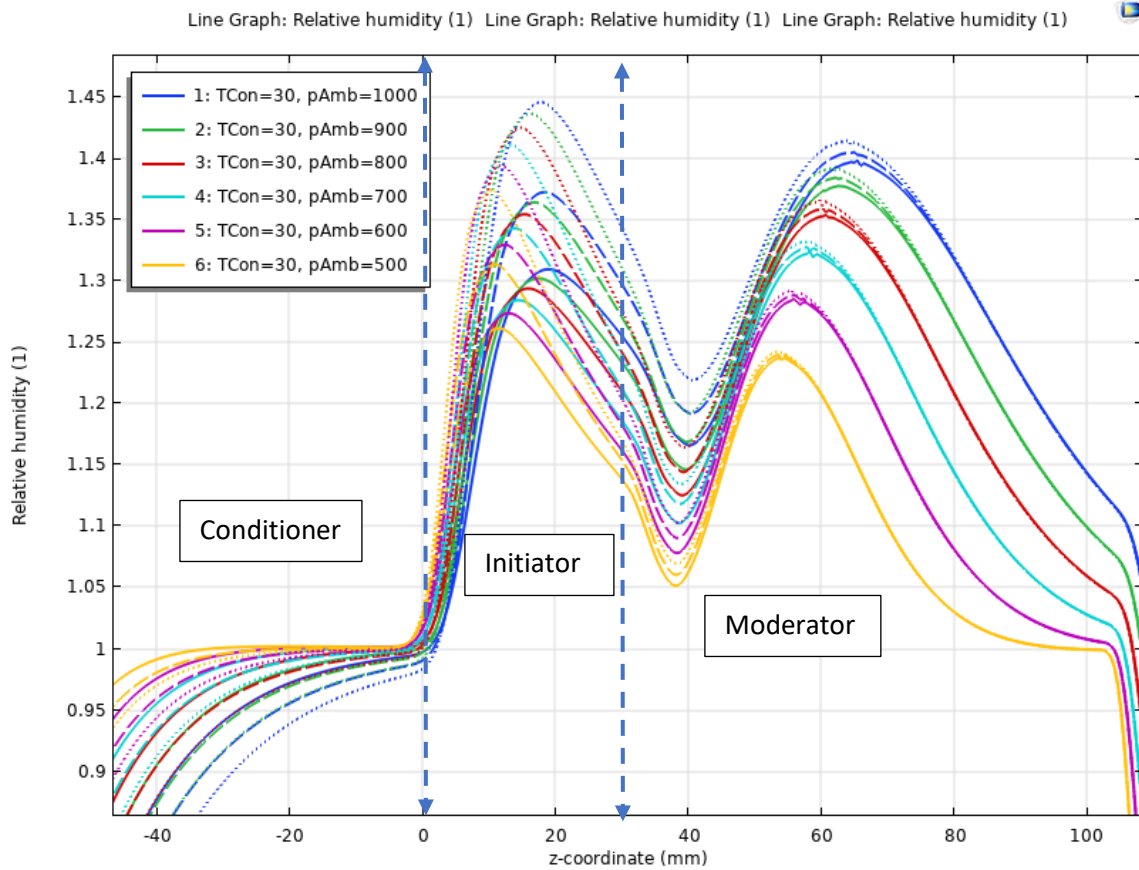


Fig. S2. Saturation ratio calculated at the centerline under different ambient pressures for various conditioner temperatures. The solid lines are for $T_{\text{cond}} = 30^\circ\text{C}$. The dashed lines are for $T_{\text{cond}} = 27^\circ\text{C}$, and the dotted lines are for $T_{\text{cond}} = 24^\circ\text{C}$. The colors indicate pressure in the hPa.

Simplified condensation effects on droplet size inside of the initiator

Lathem and Nenes (2011) examined the supersaturation profile generated in a continuous -flow streamwise thermal-gradient growth tubing. Their work shows when water vapor depletion can have an essential impact on supersaturation under certain conditions. The depletion effects on the supersaturation (s) can be described by:

$$s = s_0 - \frac{\pi R^2 R_g T^2}{\Delta H_v G Q P_s} \dot{C} \quad (4)$$

Where T is the temperature, Q is the aerosol flow rate, R is the radius of the growth tube, P_s is the saturation pressure of the water, and assuming $dT/dz=G$, and s_0 denotes the maximum supersaturation

ratio in the instrument for "zero" particle condition. R_g is the specific gas constant for water vapor. ΔH_v is the enthalpy of evaporation of water, \dot{C} describes the condensational loss (Seinfeld and Pandis, 2016).

The depletion effect leads to a lower supersaturation (s), hence lower the droplet size at the exit of the growth tubing (Nenes and Seinfeld, 2003; Seinfeld and Pandis, 2016).

$$D_p^2 = D_{p0}^2 - 2 \int \Gamma \frac{\pi R^2 R_g T^2}{\Delta H_v G Q P_s} \dot{C} dt \quad (5)$$

Where D_{p0} is the average droplet size at "zero" particle concentration for $\dot{C} \rightarrow 0$.

Γ is a growth parameter that depends on the droplet size and the water vapor mass transfer coefficient (Seinfeld and Pandis, 2016)

$$\Gamma = \frac{1}{\frac{\rho_w R T_\infty}{4 P_{sat} \Gamma D_{va} P' M_w} + \frac{\Delta H_v \rho_w}{4 k_a T_\infty} \left(\frac{\Delta H_v M_w}{T_\infty R} - 1 \right)} \quad (6)$$

To further simplify the equation (4) and (5), more convenient forms can be derived if \dot{C} is explicitly written as a function of D_p , N , and Γ . The average droplet size $\overline{D_p} = (1/N) \sum_n N_i D_{pi}$.

$$\dot{C} = \frac{\pi R^* T \rho_w}{2 M_w} \Gamma N \overline{D_p} s \quad (7)$$

If we assume $\Phi = \frac{\pi^2 R^2 R_g R^* T^3 \rho_w}{\Delta H_v G Q P_s M_w}$, equation (4) can be simplified as

$$\frac{s}{s_0} = \frac{1}{1 + \frac{\Phi}{2} \Gamma N \overline{D_p}} \quad (8)$$

Where R^* , M_w , ρ_w are the universal gas constant (8.314 J/mol/K), the molecular weight and density of liquid water.

The simplification of the droplet size depression equation results from equation (5) and (6)

$$\frac{D_p}{D_{p0}} = \left(1 + \Phi \Gamma N \overline{D_p} \right)^{-1/2} \quad (9)$$

The value of the thermal accommodation coefficient (α_T) is uncertain and was set to equal to the mass accommodation coefficient (α_c) in this simplified analysis. The value of α_c was varied from 1 for rapidly activating aerosol to 0.01, which for slowly activating aerosol. However, based on the estimation, this variation did not significantly affect the saturation and droplet size, as shown in Fig. 3. Additionally, reducing the conditioner temperature also has influenced (<20% with the 15% reduction of s) the saturation profile. Previous studies showed that the droplet size exiting the moderator tube might have up to 90% particle loss if the droplet size is larger than 10 μm (Chen and Pui, 1995; Fletcher et al., 2009; Takegawa and Sakurai, 2011). Meanwhile, the signal-to-noise ratio is too high for small droplets. Thus, this simulation assumed the droplet size exiting the initiator is between 1 to 7 μm .

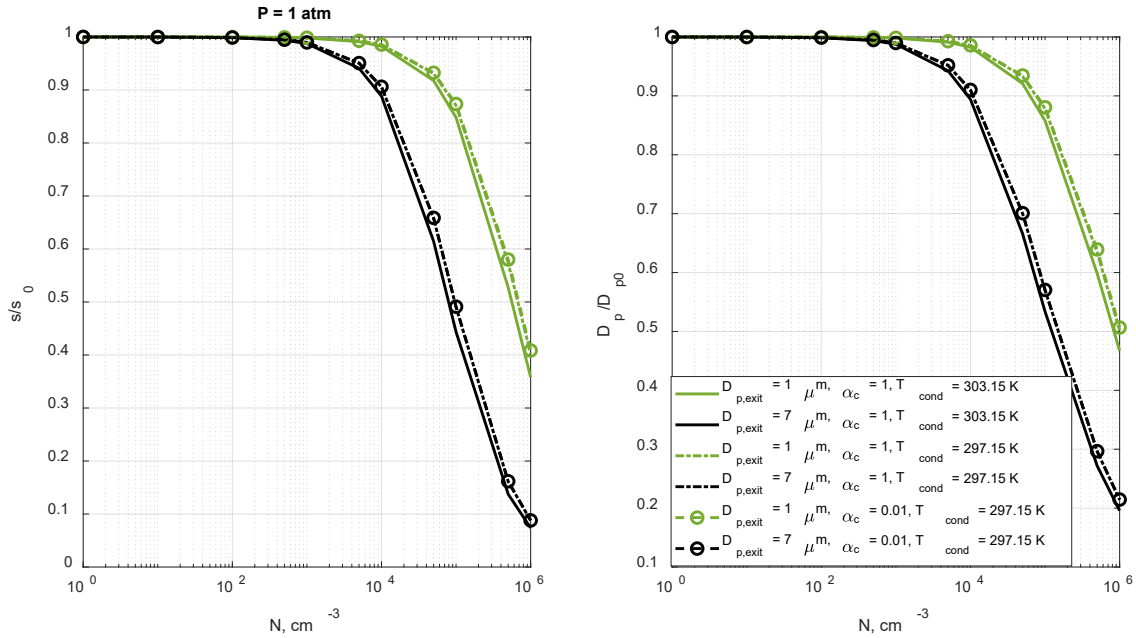


Fig. S3. Predicted supersaturation depletion and droplet size depression ratio as a function of aerosol number concentration. Results are shown for different mass accommodation coefficients and conditioner setting temperatures.

The wCPC monitors the height of the pulses generated in the optical detector and reports a status parameter to indicate the percentage of the sampled particles, which have an acceptably high pulse. Although the exact droplet size detected by the detector is unknown, this pulse height parameter indirectly shows insufficient particle growth in the detector chamber.

The saturation depletion and the droplet size depression function as the aerosol number concentration at the ambient condition (1 atm), as shown in Fig. 3. The 10% reduction of s and D_p is predicted for $N_{1\mu\text{m}} \sim 6 \times 10^4 \text{ (cm}^{-3}\text{)}$, the mean droplet size at the initiator's exit is $1 \mu\text{m}$ with the conditioner temperature setting is $30 \text{ }^\circ\text{C}$. Under the same temperature setting, if the mean droplet size at the exit of the initiator should be $7 \mu\text{m}$ to make sure the detector counts the particles, the 10% reduction of s and D_p happened when the $N_{7\mu\text{m}} \sim 8.5 \times 10^3 \text{ (cm}^{-3}\text{)}$. With the conditioner's temperature decreased to $24 \text{ }^\circ\text{C}$, the threshold concentration ($N_{1\mu\text{m}}$ and $N_{7\mu\text{m}}$) for the 10% reduction of s and D_p increased about 15% ($N_{1\mu\text{m}} \sim 7 \times 10^4 \text{ (cm}^{-3}\text{)}$ and $N_{7\mu\text{m}} \sim 1 \times 10^4 \text{ (cm}^{-3}\text{)}$) from the concentration values under the $30 \text{ }^\circ\text{C}$ conditioner temperature. Thus, the droplet size at the initiator's exit determines the aerosol number concentration limits due to the saturation depletion and the droplet size depression.

The simulation results shown in Fig. S3 suggest that the droplet size at the initiator's exit should be larger than $3 \mu\text{m}$ under the low-pressure. We examined the effect of the operating pressure on the 10% reduction threshold theoretically, as shown in Fig. S4. The theoretical analysis suggests that the 10% reduction threshold ($N_{3\mu\text{m}}$) is about $1.94 \times 10^4 \text{ (cm}^{-3}\text{)}$ at 1 atm, when the conditioner temperature is $24 \text{ }^\circ\text{C}$. Based on the theoretical analysis, with the decrease of the operating pressure, the 10% reduction threshold of $N_{3\mu\text{m}}$ reduced about 5% of the aerosol concentration ($1.85 \times 10^4 \text{ (cm}^{-3}\text{)}$) at 0.5 atm.

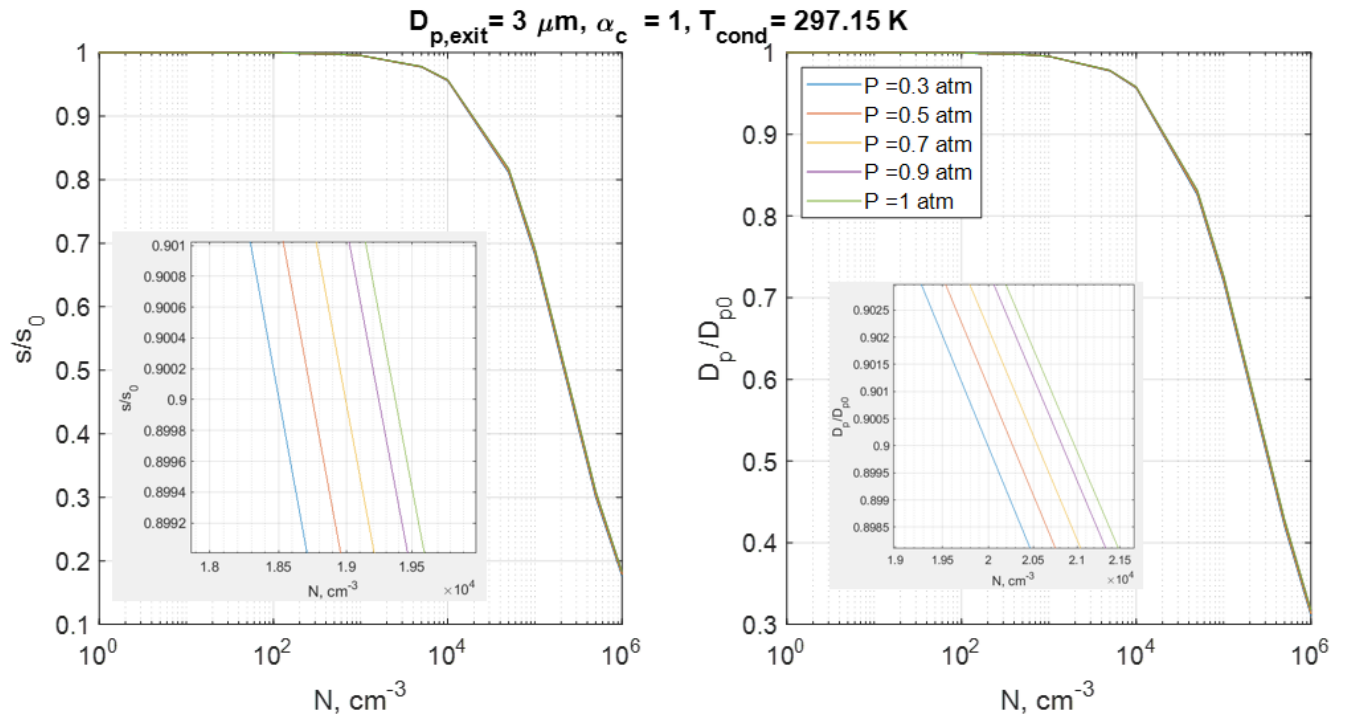
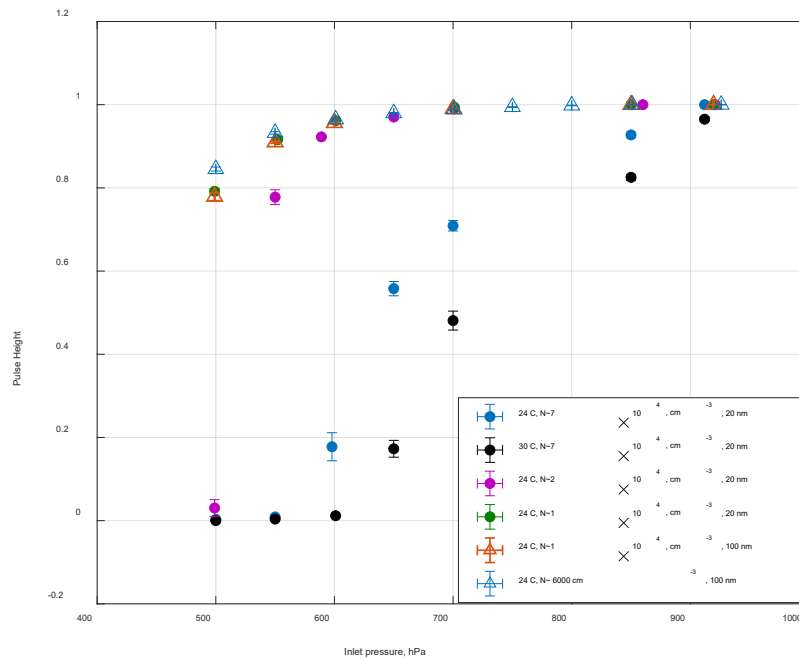
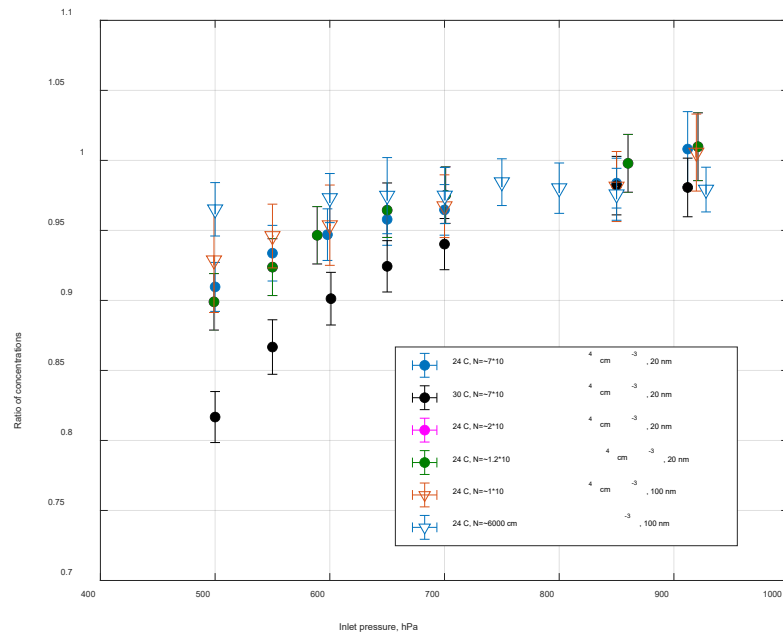


Fig. S4. Predicted supersaturation depletion and droplet size depression ratio as a function of aerosol number concentration. Results are shown for the droplet size is 3 mm when the droplet exit the initiator and the conditioner temperature is 24 °C.



(a)



(b)

Fig. S5. The water depletion due to the aerosol number concentration, illustrated by (a) the pulse height generated in the optical detector, (b) the counting efficiency as a function of the inlet pressure. Results are shown with the conditioner temperatures were set at 24 °C and 30 °C, with the initiator temperature is 59 °C and the moderater temperature is 10 °C.

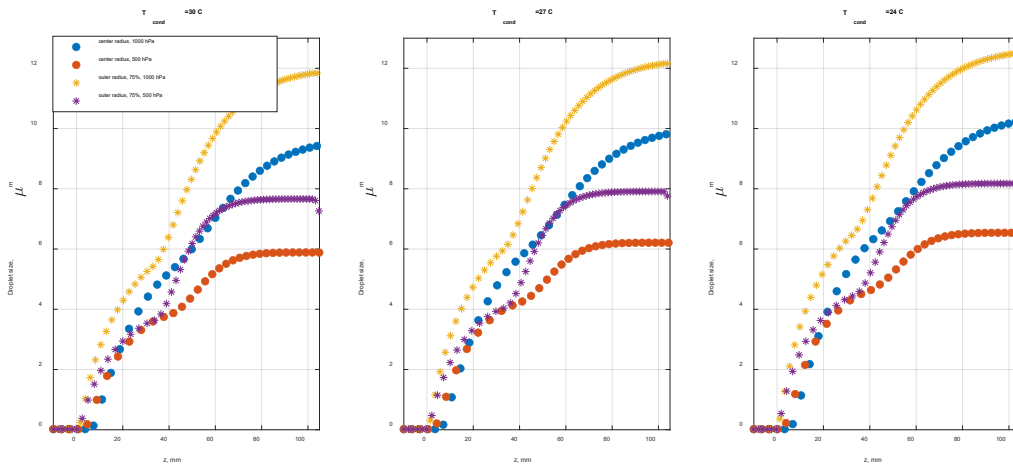


Fig. S6. Predicted droplet size evolution along the growth tube of the CPC 3789 under the different conditioner temperatures (30 °C, 27 °C, and 24 °C), with the initiator temperature is 59 °C and the moderater temperature is 10 °C. Starting particle size is 20 nm.

Table S1. Properties of tested aerosol particles.

| Properties | Ammonium sulfate | PSL | Sucrose | Humic acid | Oleic acid | Water |
|------------------------------|---|---|---|---|---|---|
| Molecular weight (g/mol) | 132.14 | N/A | 342.3 | 227.17 | 282.47 | 18.02 |
| Melting point | 235 °C | 100-110 °C* | 186 °C | 300 °C | 13.4 °C | 0 °C |
| Density (g/cm ³) | 1.77 | 1.055 (20 °C) | 1.59 | 1.77 | 0.895 | 0.997 (20 °C) |
| Water solubility | 70.6 g/100 g water | insoluble | greater than or equal to 100 mg/mL at 66° F | insoluble | insoluble | N/A |
| Reference | https://en.wikipedia.org/wiki/Ammonium_sulfate | https://www.thermofisher.com | https://pubchem.ncbi.nlm.nih.gov/compound/Sucrose | https://pubchem.ncbi.nlm.nih.gov/compound/90472028 | https://www.britannica.com/science/oleic-acid | https://en.wikipedia.org/wiki/Water |

- Glass transition temperature